bioRxiv preprint doi: https://doi.org/10.1101/2020.04.04.025684; this version posted April 5, 2020. The copyright holder for this preprint (which was not certified by peer review) is the author/funder, who has granted bioRxiv a license to display the preprint in perpetuity. It is made available under aCC-BY-NC-ND 4.0 International license.

Neural dynamics of phoneme sequencing in real speech jointly encode order and invariant content

*Laura Gwilliams[1, 2], Jean-Remi King[1, 3], †Alec Marantz[1, 2, 4] & †David Poeppel[1, 5]
[1]Department of Psychology, New York University,
[2]NYU Abu Dhabi Institute,
[3]École normale supérieure,
[4]Department of Linguistics, New York University,
[5]Max Planck Institute

Abstract

Listeners experience speech as a sequence of discrete words. However, the real input is a continuously varying acoustic signal that blends words and phonemes into one another. Here we recorded two-hour magnetoencephalograms from 21 subjects listening to stories, in order to investigate how the brain concurrently solves three competing demands: 1) processing overlapping acoustic-phonetic information while 2) keeping track of the relative order of phonemic units and 3) maintaining individuated phonetic information until successful word recognition. We show that the human brain transforms speech input, roughly at the rate of phoneme duration, along a temporally-defined representational trajectory. These representations, absent from the acoustic signal, are active earlier when phonemes are predictable than when they are surprising, and are sustained until lexical ambiguity is resolved. The results reveal how phoneme sequences in natural speech are represented and how they interface with stored lexical items.

Keywords: phonology, MEG, magnetoencephalography, auditory sequences, brain, language

One sentence summary

The human brain keeps track of the relative order of speech sound sequences by jointly encoding content and elapsed processing time

* Correspondence to: leg5@nyu.edu
† Denotes equal contribution

bioRxiv preprint doi: https://doi.org/10.1101/2020.04.04.025684; this version posted April 5, 2020. The copyright holder for this preprint (which was not certified by peer review) is the author/funder, who has granted bioRxiv a license to display the preprint in perpetuity. It is made available under aCC-BY-NC-ND 4.0 International license.

Speech comprehension involves mapping non-stationary, highly variable and continuous acoustic signals onto discrete linguistic representations [1]. Although the human experience is typically one of effortless understanding, the computational infrastructure underpinning speech processing remains a major challenge for neuroscience [2] and artificial intelligence systems [3] alike.

Existing cognitive models primarily serve to explain the recognition of words in isolation [4, 5, 6]. Predictions of these models have gained empirical support in terms of neural encoding of phonetic features [7, 8, 9, 10], and interactions between phonetic and (sub)lexical units of representation [11, 12, 13, 14, 15]. What is not well understood, and what such models largely ignore, however, is how sequences of acoustic-phonetic signals (e.g. the phonemes *k-a-t*) are mapped to lexical items (e.g. *cat*) during comprehension of naturalistic continuous speech.

One substantial challenge is that naturalistic language does not come pre-parsed: there are, e.g. no reliable cues for word boundaries, and adjacent speech sounds (phonemes) acoustically overlap both within and across words due to co-articulation [1]. In addition, the same sequence of phonemes can form completely different words (e.g. *pets* versus *pest*), so preserving phoneme order is critical. Furthermore, phonemes elicit a *cascade* of neural responses, which long surpass the duration of the phonemes themselves [16, 17, 9]). This means, concretely, that a given phoneme$_i$ is still present in both the acoustic and neural signals while subsequent phonemes stimulate the cochlea. Such signal complexity presents serious challenges for the key goals of achieving invariance and perceptual constancy in spoken language comprehension.

Based on decoding analyses of acoustic and neural data we show how the brain orchestrates these overlapping inputs and overlapping neural processes, without confusing either the content or order of the phoneme sequences. We address how the language system (i) simultaneously processes acoustic-phonetic information of overlapping inputs; (ii) keeps track of the relative order of those inputs; and (iii) maintains information sufficiently long enough to interface with (sub)lexical representations.

1. Results

Neural responses were recorded with magnetoencephalography (MEG) while 21 participants listened to four short stories. Each subject completed two one-hour recording sessions, yielding brain responses to ~50,000 phonemes, ~10,000 words and ~1,000 sentences per subject (see Figure 1A).

1.1. Phonetic feature encoding in acoustic and neural signals

First we tested when and how linguistic features of the speech input are encoded in acoustic (spectro-temporal) and neural (MEG) signals. To this aim, we fit a ridge regression to decode 14 phonetic features (one-hot encoding of three distinctive features *place, manner* and *voicing*), either from 50 frequency bands of the acoustic spectrogram (acoustic analysis) or from the 208 MEG channels (neural analysis). Using a 25-split cross validation loop, the model was trained on responses to all phonemes from the training set, and then tested as a function of their relative position in the words.

Figure 1B shows the outcome of these analyses. Although the average phoneme duration is less than 80 ms (mean duration = 78 ms; SD = 34 ms), phonetic features (averaged over position) can be decoded from the acoustic signal between 0-300 ms ($p < .001$; $\hat{t} = 9.56$), and between 50-300 ms in the neural signal ($p < .001$; $\hat{t} = 3.61$). This confirms that featural cues extend

bioRxiv preprint doi: https://doi.org/10.1101/2020.04.04.025684; this version posted April 5, 2020. The copyright holder for this preprint (which was not certified by peer review) is the author/funder, who has granted bioRxiv a license to display the preprint in perpetuity. It is made available under aCC-BY-NC-ND 4.0 International license.

to neighbouring phonemes. The ability to decode such phonetic features from the spectrum of the acoustics shows the existence of putatively invariant acoustic cues, which sufficiently generalise across phoneme locations [18, 19]. Furthermore, phonetic features that were more strongly encoded in the acoustic signal were also better decoded from the neural signal (Spearman correlation $r = .59$; $p = .032$; note that the large difference in decoding accuracy between acoustic and brain signals is expected given the signal-to-noise ratio of single-trial MEG recordings).

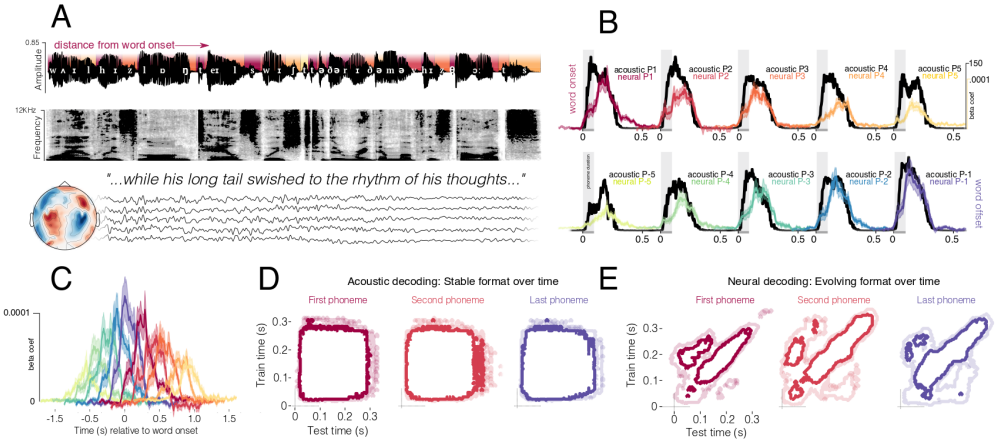

Figure 1: **Experimental design and acoustic-phonetic analysis.** A: Example sentence from the stories, with the parse into phonological units superimposed on the acoustic waveform. Colours of the segments at the top half of the waveform indicate the phoneme's distance from the beginning of a word (darker red at word onset). The spectrogram of the same sentence appears below the waveform. Five example sensor time-courses are shown below, indicating that all recordings of the continuous stories were recorded with continuous concurrent MEG. B: Time-course of phonetic-feature decoding accuracy. Black lines show accuracy of decoding features from the acoustic spectrogram. Coloured lines show results when decoding the same features from the MEG sensors. Shading in the neural data corresponds to the standard error of the mean across subjects. Results are plotted separately for 10 different phoneme positions, where P1:P5 indicates distance from word onset and P-1:P-5 distance from word offset. All plots share the same y-axis scales, which are different for neural and acoustic analyses (top right). C: The same neural decoding data are here overlaid, relative to the average duration between one phoneme and the next (around 80 ms). Multiple phonemes can be read out from the neural signal at the same time. D: Results of the temporal generalisation (TG) analysis on the acoustic data. The y-axis corresponds to the time that the decoder was trained, relative to phoneme onset; the x-axis corresponds to the time that the decoder was tested, relative to phoneme onset. The results are shown separately for three different phoneme positions. Contours represent 95% and 90% percentile decoding accuracy. E: Results of the same TG analysis applied to the MEG data, showing a very different dynamic profile from the acoustic analysis. Contours represent 95% and 90% percentile decoding accuracy.

1.2. Rapidly evolving neural representations

On average, phonetic features were linearly decodable for three times longer than the duration of the phoneme itself. This suggests that, at any one time, three phonemes are being processed concurrently (Figure 1C). How does the brain implement this set of parallel computations and prevent interference between the resulting content?

We tested whether the pattern of neural activity (from the MEG analysis) or the combination of spectro-temporal features (from the acoustic analysis) remained stable with respect to discriminability using temporal generalisation analysis [20]. This reveals whether a given representation evolves or is transformed during processing.

bioRxiv preprint doi: https://doi.org/10.1101/2020.04.04.025684; this version posted April 5, 2020. The copyright holder for this preprint (which was not certified by peer review) is the author/funder, who has granted bioRxiv a license to display the preprint in perpetuity. It is made available under aCC-BY-NC-ND 4.0 International license.

For the acoustic analysis (Figure 1D), there was significant generalisation, leading to no statistical differences between the accuracy time-course of a single decoder, as compared to independent decoders at each time sample (p = .51; $\hat{t}$ = -.67). This 'square' temporal generalisation suggests that although the acoustic signals are transient and dynamic, they contain stationary cues for acoustic-phonetic features. By contrast, the underlying representations of neural information evolved rapidly over time (Figure 1E). Concretely, any particular topographic pattern was informative to read out a phonetic feature for around 80 ms, whereas the duration of the entire dynamic process lasted around 300 ms. This was confirmed using an independent samples t-test, comparing diagonal and horizontal decoding performance ($p < .001$; $\hat{t} = 7.54$). Neural and acoustic dynamics did not change as a function of phoneme position.

Practically speaking, that the neural responses show a diagonal rather than square generalisation pattern means the underlying activations are evolving over time: activity supporting the processing of a particular phonetic feature is either moving across cortical regions or evolving or transforming within a particular cortical region.

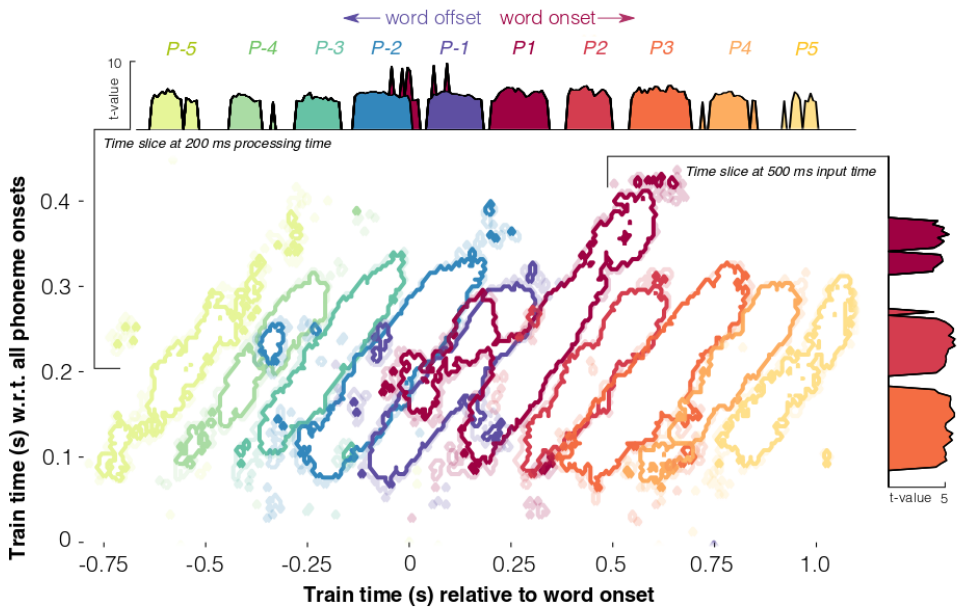

Figure 2: **Phonetic feature processing across the sequence.** Temporal generalisation (TG) results superimposed for 10 phoneme positions. From word onset (P1, dark red), and from word offset (P-1, dark blue). The result for each phoneme position is shifted by the average duration from one phoneme to the next. The y-axis corresponds to the time that the decoder was trained, relative to phoneme onset. The x-axis corresponds to the time that the decoder was tested, relative to (superimposed) word onset. Contours represent a t-value threshold of 4 (darker lines) and 3.5 (lighter lines). The panel at the top shows the t-values for each phoneme at a training time of 200 ms, showing that there is no representational overlap between neighbouring phonemes. The panel on the right shows a slice of time at 500 ms after the onset of the first phoneme. This shows that at a single moment relative to input time, multiple (at least three) phonemes can be read out of the neural responses.

bioRxiv preprint doi: https://doi.org/10.1101/2020.04.04.025684; this version posted April 5, 2020. The copyright holder for this preprint (which was not certified by peer review) is the author/funder, who has granted bioRxiv a license to display the preprint in perpetuity. It is made available under aCC-BY-NC-ND 4.0 International license.

1.3. Phonetic sequence processing

The above results show that while multiple phonemes are represented simultaneously in the brain, their dynamic encoding scheme may minimise the overlap between neighbouring representations. To test this hypothesis, we aligned the temporal generalisation matrices relative to the average latency between two adjacent phonemes. For example, relative to word onset, phoneme P1 is plot at t=0, P2 at t=80, P3 at t=160, etc. We extracted the time-samples that exceeded a $p <$ .05 threshold, Bonferroni-corrected across the 201 time-samples of a single processing time. We then computed the relative overlap between the time-samples of one phonemic unit and another. As shown in Figure 2, there is virtually no overlap when the data are examined at a particular processing time (horizontal axis). Crucially, this suggests that although multiple phonemes are processed in parallel, any given pattern of neural activity only represents one phoneme at a time, allowing each phoneme an individuated representation.

1.4. Representations are stable for the phoneme duration

Although the results show a clear evolution of representational format, each underlying neural pattern remained stable for ~80 ms, i.e. average phoneme duration. To test whether this maintenance scales with phoneme duration, we grouped trials into quartiles, and analysed brain responses to the shortest and longest phonemes (~4500 trials in each bin; mean duration 45 and 135 ms). Phoneme duration correlated with the duration of temporal generalisation across training time: longer phonemes generalised for an average 56 ms longer than shorter phonemes ($p =$ .005; $\hat{t} =$ -2.6) (Figure 3A).

1.5. Representations are shared across phoneme positions: invariance

Next we tested whether the same representational transformation is applied regardless of phoneme position. For this, we trained a classifier on the phonetic features of word onset phonemes and then tested this decoder on responses to the second, third and last phonemes (Figure 3B). We could read out the features of all three phoneme positions from 20-270 ms ($p <$ .001; $\hat{t} =$ 3.3), with comparable performance, thus supporting the position-invariant encoding of phonetic features.

1.6. Phonetic processing is modulated by word boundaries

How does the brain interface phonemic sequences with (sub)lexical representations (morphemes or words)? To address this issue, we evaluated decoding performance at word boundaries: word onset (position P1) and word offset (position P-1) separately for each family of phonetic features (place of articulation, manner, and voicing) (Figure 3C).

Phonetic features were decodable earlier at word onset then offset, yielding a significant difference during the first 250 ms (place: $p =$ .03, $\hat{t} =$ 2.77, 84-112 ms; $p <$ .001, $\hat{t} =$ -2.8, 156-240 ms; manner $p <$ .001, $\hat{t} =$ 3.03, 72-196 ms; $p =$ .004, $\hat{t} =$ 2.75, 220-300ms). The latency between average neural and acoustic maximum accuracy was 136 ms (SD = 13 ms) at word onset and 4 ms (SD = 13 ms) at word offset (see Figure 1B), leading to a significant difference between onset and offset phonemes averaged over phonetic features ($t =$ -3.08; $p =$ .002). Furthermore, place and voicing features were sustained in the neural signal significantly longer for phonemes at the beginning of words as compared to the end (place: $p =$ .009, $\hat{t} =$ -3.05, 302-418 ms; voicing: $p <$ .001, $\hat{t} =$ -3.76, 328-428 ms). This was also true when averaging over all features ($p <$ .001, $\hat{t} =$ -3.79, 328-396 ms) (see Figures 1B and 2).

bioRxiv preprint doi: https://doi.org/10.1101/2020.04.04.025684; this version posted April 5, 2020. The copyright holder for this preprint (which was not certified by peer review) is the author/funder, who has granted bioRxiv a license to display the preprint in perpetuity. It is made available under aCC-BY-NC-ND 4.0 International license.

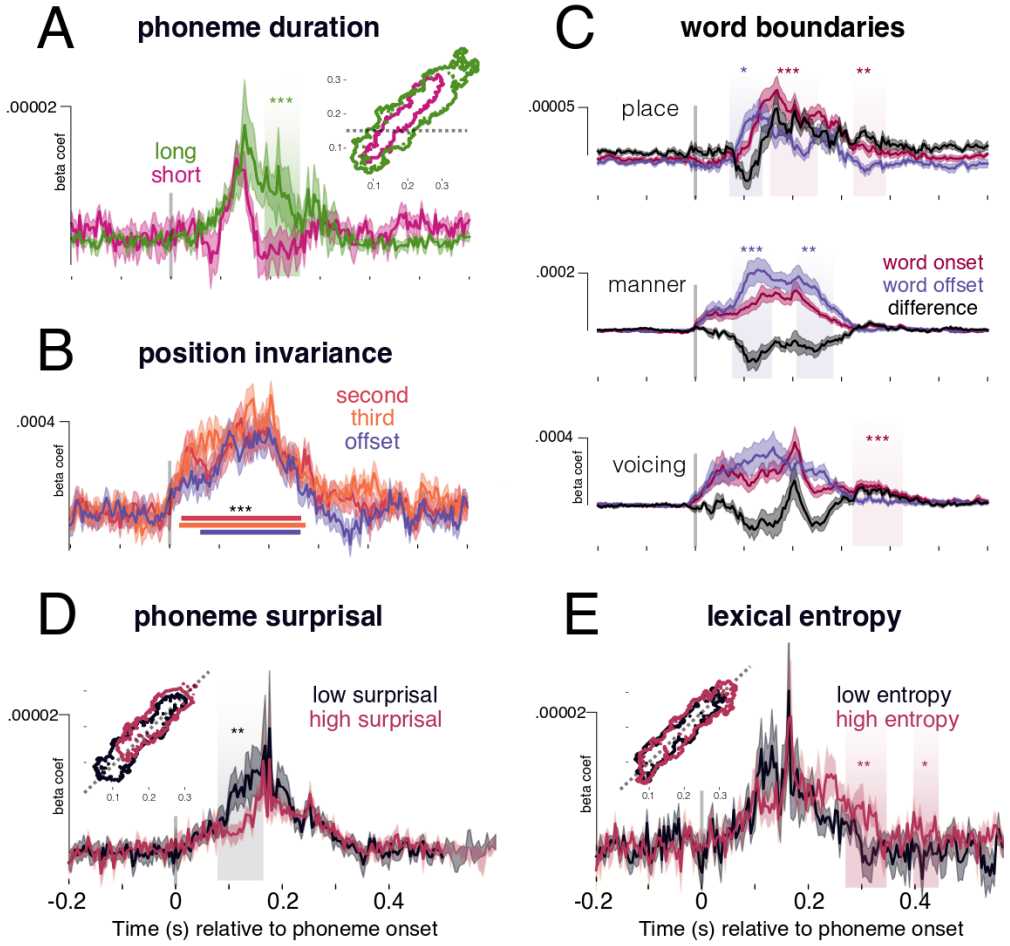

Figure 3: **Elucidating sequence dynamics.** A: TG analysis median split into short (average 45 ms) and long (average 135 ms) phonemes. Contour inlay represents the borders of the significant clusters at $p < .001$. Waveforms represent a horizontal slice at 140 ms (shown as a dashed line in the contour plot). B: Decoding performance when training on responses to word onset, and evaluating on second, third and last phoneme in the word. Lines represent against-chance temporal clusters exceeding $p < .001$ for the three phoneme positions. C: Analysing responses along the diagonal plane for phonemes at word onset (dark red) and offset (dark blue) and their subtraction (black), split into the three families of phonetic features. Coloured shading corresponds to significant clusters found using applying a temporal cluster test to the difference wave. D: Analysis on all non-onset phonemes split into median surprisal, along the diagonal plane (slice shown in contour plot). Highlighted areas show significant temporal clusters between low and high surprisal. E: Analysis on all non-onset phonemes split into median cohort entropy, also along the diagonal plane. Highlighted areas show significant temporal clusters between low and high entropy. Shading on the waveform of all plots represents standard error of the mean across subjects. * = $p < .05$; ** = $p < .01$; *** = $p < .001$.

1.7. Predictable phonemes are processed earlier

We hypothesised that the latency shift observed at word boundaries may be due to the predictability of each phoneme. Specifically, we tested whether expected phonemes could be de-

bioRxiv preprint doi: https://doi.org/10.1101/2020.04.04.025684; this version posted April 5, 2020. The copyright holder for this preprint (which was not certified by peer review) is the author/funder, who has granted bioRxiv a license to display the preprint in perpetuity. It is made available under aCC-BY-NC-ND 4.0 International license.

coded earlier from the neural signal than surprising ones. To control for co-linearity between word-boundaries and surprisal, we selected all phonemes that were *not* at word onset, and tested decoding accuracy as a function of quartile phoneme surprisal (see Methods for details on how this variable was computed). Each analysis bin contained ~4500 trials, with a mean surprisal of 0.12, 1.38, 2.8 and 5.16 bits.

There was a systematic latency shift as a function of non-onset phoneme surprisal (Figure 3D): more predictable phonemes were decoded earlier than less predictable ones, leading to a significant difference between low and high surprisal from 120-132 ms (p = .007). Surprisal did not significantly modulate peak decoding accuracy (all uncorrected p-values > .2).

1.8. Phonetic features are maintained until lexical identification

Finally, to investigate whether phonetic representations are maintained until word recognition, we test two hypotheses: (i) phonetic features are maintained until the identification of a word boundary; or (ii) they are maintained until certainty about word identity surpasses a particular threshold. We evaluated whether decoding performance between 300-420 ms (the window that showed the word onset/offset effect) was better explained by word length or by word certainty (entropy over possible lexical candidates).

For (i), we compared decoding performance of word-onset phonemes, grouped into median word length (shorter mean length = 2.54 phonemes; 4058 trials; longer mean length = 5.2 phonemes; 2841 trials). No significant differences between groups were found (all clusters p > .2, duration < 2 ms). For (ii), we grouped trials based on non-onset cohort entropy, and ran the analysis on all phonemes that did *not* occur at word onset (~4500 trials per bin, mean values of 0.03, 0.77, 2.04 and 4.48 bits). In the window of interest, higher entropy phonemes we decoded with significantly higher performance (304-328 ms, p = .002, $\hat{t}$ = -2.12) (see Figure 3E). This suggests that phonetic information is maintained for longer in cases of higher lexical uncertainty.

2. Discussion

How is the rapidly unfolding speech signal transformed into a sequence of discrete linguistic units? We analysed MEG responses to continuous speech, as a function of phonetic features and position in the phoneme sequence. Our results show that although both acoustic cues and neural processes overlap in time (lasting around 300 ms), the underlying representation evolves at the phonemic unit rate (around 80 ms), thus ensuring non-overlapping representations to avoid interference. Furthermore, we demonstrate that features are processed earlier when the phoneme is predictable – and then maintained until lexical identity is resolved. Taken together, our results show that a highly dynamic and adaptive language system underpins phonological and lexical processing during naturalistic listening.

The stationarity of the acoustic signal *versus* the dynamics of the corresponding neural representations highlight that speech driven-responses are more than just a reflection of the acoustic signals [21]. These dynamical representations allow the brain to process multiple (at least three) successive phonemes simultaneously, without blending them within a common activity pattern. This grants two computational advantages. First, it serves to avoid interference between phonetic units, by ensuring an orthogonal format in processing space. This answers the key question of how overlapping sequences are maintained without confusing the content of the signal. Second, relative position is implicitly coded in the representational format of each phoneme at a given input time. This allows the system to keep track of the order of speech sounds, i.e. to know that you were asked to *teach* and not *cheat*, or that you are eating *melons* and not *lemons*.

bioRxiv preprint doi: https://doi.org/10.1101/2020.04.04.025684; this version posted April 5, 2020. The copyright holder for this preprint (which was not certified by peer review) is the author/funder, who has granted bioRxiv a license to display the preprint in perpetuity. It is made available under aCC-BY-NC-ND 4.0 International license.

Building on this observation, we found that the representational trajectory is consistent across phoneme positions, thus leading to significant generalisation from one phoneme position to another, with comparable magnitude. Although a simple result, this rules out a number of competing hypotheses. First, it is hard to reconcile these results with an explicit sequence representation. For example, if the brain represents a sequence of all elapsed phonemes, the representation of phoneme *X* at word onset would generalise poorly to third position *ABX* and even worse to sixth position *ABCDEX*. Second, under the same logic, this result rules out the idea that phonemes have a context-dependent encoding scheme, such as being represented along with their co-articulatory neighbours [22]. In that case, phoneme *X* would have a different representation in the context *AXB* and *VXY*. Finally, generalisability is inconsistent with position-specific encoding accounts, such as edge-based schemes [23, 24], which would posit that *X* is encoded differently in *ABX* and *XBC*. Instead, our results support a context-independent account, which encodes distance from phoneme onset, regardless of lexical edges.

If all phonemes follow a common representational trajectory relative to phoneme onset, how can we describe the transformational space? One possibility links to articulatory phonology [25]. Although we showed the input acoustic space to be (surprisingly) static, the articulatory gestures which produce those acoustics are inherently dynamic [26]. It is plausible, therefore, that speech sounds are processed via articulatory commands, which are believed to jointly encode both the sound being produced and the temporal delay relative to articulatory onset. This idea of joint content-temporal coding resonates with recent findings of sequence encoding – finding evidence for dedicated temporal codes in rat hippocampus [27]. Future work will need to further delineate the temporal code used for phonological processing, and how the spatial location of these responses changes as a function of processing time.

A critical finding is that the representational trajectory gets systematically delayed as a function of phonological uncertainty (surprisal) and systematically sustained as a function of lexical uncertainty (cohort entropy). This suggests that the language system continuously adapts its processes based on information across multiple levels of linguistic description simultaneously.

The latency shift for more predictable phonemes straightforwardly aligns with models of predictive coding [28, 29] and analysis-by-synthesis [30]: when predictability for a phoneme is strong, processes can be initiated earlier (perhaps in some cases before the sensory input) than when the phoneme identity is unknown. Although previous work has shown that processing of the speech signal is sensitive to phoneme probability within a word [31, 11, 13, 14, 32], this is the first study quantifying the *consequences* this has for encoding the content of those phonemes. Interestingly, we did not observe an effect of predictability on overall decoding performance, suggesting that processing delays may serve as a compensatory mechanism to allow more information to be accumulated in order to reach the same strength of encoding [33]. Future work should test whether this local (within-word) predictability metric has similar consequences to global (across-word) metrics.

The finding that phonetic features are maintained longer in the face of lexical ambiguity is a critical piece of the puzzle for understanding the interface between acoustic-phonetic representations and the mental lexicon. This result not only highlights the adaptivity of the speech processing system but also demonstrates the online bi-directional interaction between hierarchical levels of processing. Our results suggest that acoustic-phonetic information is maintained until the (sub)lexical identity reaches a confidence threshold. To our knowledge, this is the first evidence for active maintenance of phonetic information until statistically-defined boundaries, and has clear processing advantages in the face of phonological ambiguity and lexical revision [15].

bioRxiv preprint doi: https://doi.org/10.1101/2020.04.04.025684; this version posted April 5, 2020. The copyright holder for this preprint (which was not certified by peer review) is the author/funder, who has granted bioRxiv a license to display the preprint in perpetuity. It is made available under aCC-BY-NC-ND 4.0 International license.

Overall, our results reveal that the brain implements an elegant computational solution to the processing of rapid, overlapping phoneme sequences. Namely, that the phonetic content of the unfolding speech signal is jointly encoded with elapsed processing time. Future work will need to assess the generality of this computational framework, and whether it subserves sequence processing across other modalities and domains.

3. Method

3.1. Participants

Twenty-one native English participants were recruited from the NYU Abu Dhabi community (13 female; age: M=24.8, SD=6.4). All provided their informed consent and were compensated for their time. Participants reported having normal hearing and no history of neurological disorders. Each subject participated in the experiment twice. Time between sessions ranged from 1 day to 2 months.

3.2. Stimulus development

Four fictional stories were selected from the Open American National Corpus: Cable spool boy (about two bothers playing in the woods); LW1 (sci-fi story about an alien spaceship trying to find home); Black willow (about an author struggling with writer's block); Easy money (about two old friends using magic to make money).

Stimuli were annotated for phoneme boundaries and labels using the 'gentle aligner' from the Python module *lowerquality*. Some prior testing provided better results than the Penn Forced Aligner.

Each of the stories were synthesised using the Mac OSX text-to-speech application. Three synthetic voices were used (Ava, Samantha, Allison). Voices changed every 5-20 sentences. The speech rate of the voices ranged from 145-205 words per minute, which also changed every 5-20 sentences. The silence between sentences randomly varied between 0-1000 ms.

3.3. Procedure

Before the experiment proper, the participant was exposed to 20 seconds of each speaker explaining the structure of the experiment. This was designed to help the participants attune to the synthetic voices.

The order of stories was fully crossed using a Latin-square design. Participants heard the stories in the same order during both the first and second sessions.

Participants answered a two-choice question on the story content every ~3 minutes. For example, one of the questions was "what was the location of the bank that they robbed"? The purpose of the questions was to keep participants attentive and to have a formal measure of engagement. All participants performed this task at ceiling, with an accuracy of 98%. Participants responded with a button press.

Stimuli were presented binaurally to participants though tube earphones (Aero Technologies), at a mean level of 70 dB SPL. The stories ranged from 8-25 minutes, with a total running time of ~1 hour.

bioRxiv preprint doi: https://doi.org/10.1101/2020.04.04.025684; this version posted April 5, 2020. The copyright holder for this preprint (which was not certified by peer review) is the author/funder, who has granted bioRxiv a license to display the preprint in perpetuity. It is made available under aCC-BY-NC-ND 4.0 International license.

3.4. MEG acquisition

Marker coils were placed at five positions to localise each participant's skull relative to the sensors. These marker measurements were recorded just before and after the experiment in order to track the degree of movement during the recording.

MEG data were recorded continuously using a 208 channel axial gradiometer system (Kanazawa Institute of Technology, Kanazawa, Japan), with a sampling rate of 1000 Hz and applying an online low-pass filter of 200 Hz.

3.5. Preprocessing MEG

The raw MEG data were noise reduced using the Continuously Adjusted Least Squares Method (CALM: (Adachi et al., 2001)), with MEG160 software (Yokohawa Electric Corporation and Eagle Technology Corporation, Tokyo, Japan).

The data were bandpass-filtered between 0.1 and 50 Hz using MNE-Python's default parameters with firwin design [34] and downsampled to 250 Hz. Epochs were segmented from 200 ms pre-phoneme onset to 600 ms post-phoneme onset. No baseline correction was applied. No other data cleaning was performed.

3.6. Preprocessing auditory signals

We computed a time-frequency decomposition of the auditory signals by applying a 100-sample Hamming window to the auditory waveform. This resulted in a power estimate at each of 50 linearly spaced frequency bands from 1-11250 Hz. These data were then also downsampled to 250 Hz, and segmented from 200-600 ms in order to match the dimensionality and size of the MEG epochs.

3.7. Modeled features

We investigated whether single-trial sensor responses varied as a function of fourteen binary phonetic features, as derived from the multi-value feature system reported in [35]. Note that this feature system is sparse relative to the full set of distinctive features that can be identified in English; however, it serves as a reasonable approximation of the phonemic inventory for our purposes.

Voicing. This refers to whether the vocal chords vibrate during production. For example, this is the difference between *b* versus *p* and *z* versus *s*.

Manner of articulation. Manner refers to the way by which air is allowed to pass through the articulators during production. Here we tested five manner features: fricative, nasal, plosive, approximant, and vowel.

Place of articulation. Place refers to where the articulators (teeth, tongue, lips) are positioned during production. For vowels, this consists of: central vowel, low vowel, mid vowel, high vowel. For consonants, this consists of: coronal, glottal, labial and velar.

Nuisance variables. In the same model, we also accounted for variance explained by 'nuisance variables' – i.e. structural and statistical co-variates of the phonemes. Though we were not interested in interpreting the results of these features, we included them in the model to be sure that they did not account for our main analysis on the phonetic features. These features included: primary stress, secondary stress, frequency of the sequence, suffix onset, prefix onset, root onset, syllable location in the word, and syllable onset. These features were extracted from the English Lexicon Project [36].

bioRxiv preprint doi: https://doi.org/10.1101/2020.04.04.025684; this version posted April 5, 2020. The copyright holder for this preprint (which was not certified by peer review) is the author/funder, who has granted bioRxiv a license to display the preprint in perpetuity. It is made available under aCC-BY-NC-ND 4.0 International license.

Subset variables. Throughout the analysis, we subset trials based on their relationship to: word onset, word offset, surprisal, entropy, distance from onset, distance from offset.

Surprisal is given as:

$$P(w|C) = \frac{f(w)}{\sum_{w \in C} f(w)} \tag{1}$$

and cohort entropy is given as:

$$-\sum_{w \in C} P(w|C) log_2 P(w|C) \tag{2}$$

where C is the set of all words consistent with the heard sequence of phonemes thus far, and $f(w)$ is the frequency of the word w. Measures of spoken word frequency were extracted from the English Lexicon Project [36].

3.8. Decoding

Decoding analyses were performed separately on the acoustic signal and on the neural signal. For the acoustic decoding, the input features were the power estimates at each of the 50 frequency bands from 1-1125 Hz. For the neural decoding, the input features were the magnitude of activity at each of the 208 MEG sensors. This approach allows us to decode from multiple, potentially overlapping, neural representations, without relying on gross modulations in activation strength [37].

Because some of the features in our analysis are correlated with one another, we need to jointly evaluate the accuracy of each decoding model relative to its performance in predicting all modelled features, not just the target feature of interest. This is because, if evaluating each feature independently, we will not be able to dissociate the decoding of feature f from the decoding of the correlated feature $\hat{f}$. The necessity to use decoding over encoding models here, though (which, do not suffer so harshly from the problem of co-variance in the stimulus space) is one of signal to noise: we expect any signal related to linguistic processes to be contained in low-amplitude responses that are distributed over multiple sensors. Our chances of uncovering reliable responses to these features is boosted by using multi-variate models [37].

To overcome the issue of co-variance, but still to capitalise on the advantages of decoding approaches, we implement a back-to-back ridge regression model [38]. This involves a two stage process. First, a ridge regression model was fit on a random (shuffled) half of the data, at a single time-point. The mapping was learnt between the multivariate input (either activity across sensors or power over frequency bands) and the univariate stimulus feature (one of the 31 features described above). All decoders were provided with data normalised by the mean and standard deviation in the training set:

$$\underset{\beta}{\operatorname{argmin}} \sum_i (y_i \beta^T X_i)^2 + \alpha ||\beta||^2 \tag{3}$$

where $y_i \in \{\pm 1\}$ is the feature to be decoded at trial i and X_i is the multivariate acoustic or neural measure. The l2 regularisation parameter α was also fit, testing 20 log-spaced values from 1^{-5} to 1^5. This was implemented using the *RidgeCV* function in *scikit-learn* [39].

Then, we use the other half of the acoustic or neural responses to generate a prediction for each of the 31 features corresponding to the test set. However, because the predictions are correlated, we need to jointly-evaluate the accuracy of decoding each feature, to take into account

bioRxiv preprint doi: https://doi.org/10.1101/2020.04.04.025684; this version posted April 5, 2020. The copyright holder for this preprint (which was not certified by peer review) is the author/funder, who has granted bioRxiv a license to display the preprint in perpetuity. It is made available under aCC-BY-NC-ND 4.0 International license.

the variance explained by correlated non-target features. To do this, we fit another ridge regression model, this time learning the beta coefficients that map the matrix of *true* feature values to *predicted* feature values:

$$\underset{\beta}{\operatorname{argmin}} \sum_{i} (y_i \beta^T \hat{Y}_i)^2 + \alpha \|\beta\|^2 \tag{4}$$

where $y_i \in \{\pm 1\}$ is the ground truth of a particular stimulus feature at trial i and $\hat{Y}_i$ is the prediction for all stimulus features. A new regularisation parameter α was learnt for this stage. By including all stimulus features in the model, this accounts for the correlation between the feature of interest and the other features. From this, we use the beta-coefficients that map the true stimulus feature to the predicted stimulus feature.

The train/test split was performed 100 times, and the beta-coefficients were averaged across iterations. This circumvents the issue of unstable coefficients when modelling correlated variables. These steps were applied to each subject independently.

3.9. Temporal generalisation decoding

Temporal generalization (TG) consists of testing whether a temporal decoder fit on a training set at time t can decode a testing set at time t' [20]. This means that rather than evaluating decoding accuracy just at the time sample that the model was trained on, we evaluate its accuracy across all possible train/testing time combinations.

TG can be summarised with a square training time $\times$ testing time decoding matrix. To quantify the stability of neural representations, we measured the duration of above-chance generalization of each temporal decoder. To quantify the dynamics of neural representations, we compared the mean duration of above-chance generalization across temporal decoders to the duration of above-chance temporal decoding (i.e. the diagonal of the matrix versus its rows). These two metrics were assessed within each subject and tested with second-level statistics across subjects.

3.10. Comparing decoding performance between trial subsets

We apply analyses that rely on comparing decoding performance for different subsets of trials (e.g. between high/low surprisal, or beginning/end of word). We conduct this analysis by first training our decoding models on responses to all phonemes, thus yielding a set of fit model weights (a *topographic pattern*) at each millisecond relative to phoneme onset. We then separately evaluate the performance of these decoders on the subset trials of interest. This yields a time-course or generalisation matrix for each group of trials that we evaluate on.

3.11. Group statistics

In order to evaluate whether decoding performance is better than chance, we perform second-order statistics. This involves testing whether the distribution of beta coefficients across subjects significantly differs from chance (zero) across time using a one-sample permutation cluster test with default parameters specified in the MNE-Python package [34].

bioRxiv preprint doi: https://doi.org/10.1101/2020.04.04.025684; this version posted April 5, 2020. The copyright holder for this preprint (which was not certified by peer review) is the author/funder, who has granted bioRxiv a license to display the preprint in perpetuity. It is made available under aCC-BY-NC-ND 4.0 International license.

4. Acknowledgements

We thank Graham Flick for help with data collection. We are very grateful to William Idsardi, Arianna Zuanazzi, Joan Opella, Pablo Ripolles-Vidal and Omri Raccah for their feedback on an earlier version of the manuscript. **Funding:** This project received funding from the Abu Dhabi Institute G1001 (AM); NIH R01DC05660 (DP), European Union's Horizon 2020 research and innovation program under grant agreement No 660086, the Bettencourt-Schueller Foundation, the Fondation Roger de Spoel-berch, the Philippe Foundation (JRK) and The William Orr Dingwall Dissertation Fellowship (LG). **Author contributions:** LG: conceptualisation; methodology; software; validation; formal analysis; investigation; data curation; writing - original draft preparation and review and editing; visualisation. JRK: conceptualisation; methodology; software; supervision. AM: conceptualisation; writing - review and editing; supervision; funding acquisition. DP: conceptualisation; writing - review and editing; supervision; funding acquisition. **Competing interests:** The authors declare no competing interests. **Data and materials availability:** Preprocessed data will be made available after publication.

bioRxiv preprint doi: https://doi.org/10.1101/2020.04.04.025684; this version posted April 5, 2020. The copyright holder for this preprint (which was not certified by peer review) is the author/funder, who has granted bioRxiv a license to display the preprint in perpetuity. It is made available under aCC-BY-NC-ND 4.0 International license.

References

[1] Pisoni, D. B. & Luce, P. A. Acoustic-phonetic representations in word recognition. *Cognition* **25**, 21–52 (1987).

[2] Wöstmann, M., Fiedler, L. & Obleser, J. Tracking the signal, cracking the code: Speech and speech comprehension in non-invasive human electrophysiology. *Language, Cognition and Neuroscience* **32**, 855–869 (2017).

[3] Benzeghiba, M. *et al.* Automatic speech recognition and speech variability: A review. *Speech communication* **49**, 763–786 (2007).

[4] Marslen-Wilson, W. D. & Welsh, A. Processing interactions and lexical access during word recognition in continuous speech. *Cognitive psychology* **10**, 29–63 (1978).

[5] McClelland, J. L. & Elman, J. L. The trace model of speech perception. *Cognitive psychology* **18**, 1–86 (1986).

[6] Norris, D. Shortlist: A connectionist model of continuous speech recognition. *Cognition* **52**, 189–234 (1994).

[7] Mesgarani, N., Cheung, C., Johnson, K. & Chang, E. F. Phonetic feature encoding in human superior temporal gyrus. *Science* **343**, 1006–1010 (2014).

[8] Chang, E. F. *et al.* Categorical speech representation in human superior temporal gyrus. *Nature neuroscience* **13**, 1428 (2010).

[9] Khalighinejad, B., da Silva, G. C. & Mesgarani, N. Dynamic encoding of acoustic features in neural responses to continuous speech. *Journal of Neuroscience* **37**, 2176–2185 (2017).

[10] Yi, H. G., Leonard, M. K. & Chang, E. F. The encoding of speech sounds in the superior temporal gyrus. *Neuron* **102**, 1096–1110 (2019).

[11] Gwilliams, L. & Marantz, A. Non-linear processing of a linear speech stream: The influence of morphological structure on the recognition of spoken arabic words. *Brain and language* **147**, 1–13 (2015).

[12] Leonard, M. K., Baud, M. O., Sjerps, M. J. & Chang, E. F. Perceptual restoration of masked speech in human cortex. *Nature communications* **7**, 1–9 (2016).

[13] Gwilliams, L., Poeppel, D., Marantz, A. & Linzen, T. Phonological (un) certainty weights lexical activation. *arXiv preprint arXiv:1711.06729* (2017).

[14] Brodbeck, C., Hong, L. E. & Simon, J. Z. Rapid transformation from auditory to linguistic representations of continuous speech. *Current Biology* **28**, 3976–3983 (2018).

[15] Gwilliams, L., Linzen, T., Poeppel, D. & Marantz, A. In spoken word recognition, the future predicts the past. *Journal of Neuroscience* **38**, 7585–7599 (2018).

[16] Picton, T. W., Woods, D. L., Baribeau-Braun, J. & Healey, T. M. Evoked potential audiometry. *J Otolaryngol* **6**, 90–119 (1977).

[17] Näätänen, R. & Picton, T. The n1 wave of the human electric and magnetic response to sound: a review and an analysis of the component structure. *Psychophysiology* **24**, 375–425 (1987).

[18] Stevens, K. N. & Blumstein, S. E. Invariant cues for place of articulation in stop consonants. *The Journal of the Acoustical Society of America* **64**, 1358–1368 (1978).

[19] Blumstein, S. E. & Stevens, K. N. Acoustic invariance in speech production: Evidence from measurements of the spectral characteristics of stop consonants. *The Journal of the Acoustical Society of America* **66**, 1001–1017 (1979).

[20] King, J. & Dehaene, S. Characterizing the dynamics of mental representations: the temporal generalization method. *Trends in cognitive sciences* **18**, 203–210 (2014).

[21] Daube, C., Ince, R. A. & Gross, J. Simple acoustic features can explain phoneme-based predictions of cortical responses to speech. *Current Biology* **29**, 1924–1937 (2019).

[22] Wickelgren, W. A. Short-term memory for phonemically similar lists. *The American Journal of Psychology* **78**, 567–574 (1965).

[23] Glasspool, D. W. & Houghton, G. Serial order and consonant–vowel structure in a graphemic output buffer model. *Brain and language* **94**, 304–330 (2005).

[24] Fischer-Baum, S. A common representation of serial position in language and memory. In *Psychology of Learning and Motivation*, vol. 68, 31–54 (Elsevier, 2018).

[25] Ohala, J. J., Browman, C. P. & Goldstein, L. M. Towards an articulatory phonology. *Phonology* **3**, 219–252 (1986).

[26] Browman, C. P. & Goldstein, L. Articulatory gestures as phonological units. *Phonology* **6**, 201–251 (1989).

[27] MacDonald, C. J., Lepage, K. Q., Eden, U. T. & Eichenbaum, H. Hippocampal "time cells" bridge the gap in memory for discontiguous events. *Neuron* **71**, 737–749 (2011).

[28] Sohoglu, E., Peelle, J. E., Carlyon, R. P. & Davis, M. H. Predictive top-down integration of prior knowledge during speech perception. *Journal of Neuroscience* **32**, 8443–8453 (2012).

[29] Bendixen, A., Scharinger, M., Strauss, A. & Obleser, J. Prediction in the service of comprehension: modulated early brain responses to omitted speech segments. *Cortex* **53**, 9–26 (2014).

[30] Halle, M. & Stevens, K. Speech recognition: A model and a program for research. *IRE transactions on information theory* **8**, 155–159 (1962).

bioRxiv preprint doi: https://doi.org/10.1101/2020.04.04.025684; this version posted April 5, 2020. The copyright holder for this preprint (which was not certified by peer review) is the author/funder, who has granted bioRxiv a license to display the preprint in perpetuity. It is made available under aCC-BY-NC-ND 4.0 International license.

[31] Gagnepain, P., Henson, R. N. & Davis, M. H. Temporal predictive codes for spoken words in auditory cortex. *Current Biology* **22**, 615–621 (2012).

[32] Di Liberto, G. M., Wong, D., Melnik, G. A. & de Cheveigné, A. Low-frequency cortical responses to natural speech reflect probabilistic phonotactics. *Neuroimage* **196**, 237–247 (2019).

[33] Gold, J. I. & Shadlen, M. N. The neural basis of decision making. *Annual review of neuroscience* **30** (2007).

[34] Gramfort, A. *et al.* Mne software for processing meg and eeg data. *Neuroimage* **86**, 446–460 (2014).

[35] King, S. & Taylor, P. Detection of phonological features in continuous speech using neural networks (2000).

[36] Balota, D. A. *et al.* The english lexicon project. *Behavior research methods* **39**, 445–459 (2007).

[37] King, J.-R. *et al.* Encoding and decoding neuronal dynamics: Methodological framework to uncover the algorithms of cognition (2018).

[38] King, J.-R., Charton, F., Lopez-Paz, D. & Oquab, M. Discriminating the influence of correlated factors from multivariate observations: the back-to-back regression. *bioRxiv* (2020).

[39] Pedregosa, F. *et al.* Scikit-learn: Machine learning in python. *Journal of machine learning research* **12**, 2825–2830 (2011).